RSC Advances

ELECTRONIC SUPPLEMENTARY INFORMATION (ESI)

The importance of covalent coupling in the synthesis of high performance composite anodes for lithium ion batteries

Gul Zeb,[a] Peter Gaskell,[b] Young Nam Kim,[c] Ghulam Jalani,[a] Xingcheng Xiao,[c] Thomas Szkopek[b] and Marta Cerruti*[a]

[a] *Mining & Materials Engineering, McGill University, 3610 University Street, Montreal QC, H3A 0C5, Canada*
[b] *Electrical & Computer Engineering, McGill University, 3480 University Street, Montreal QC, H3A 2A7, Canada*
[c] *General Motors R&D Center, 30500 Mound Road, Warren MI, 48090, United States*
** Fax: +1 (514) 398 6878; Tel: +1 (514) 398 5496; E-mail: marta.cerruti@mcgill.ca*

SI1.Methods & Materials

Synthesis

Carboxylation of GNP

Graphene nanopowder (GNP) with an average flake size of ~10 µm and thickness of 1–3 nm was obtained from Graphene Supermarket (USA). Carboxylated GNP was synthesized via diazonium chemistry and is referred to as $^{COOH-}$GNP. The procedure involved preparing a solution of 4–aminobenzene acetic acid (1.37 g, Sigma) and sodium nitrite (0.7 g, Sigma) in 0.5M hydrochloric acid (0.1 L) to achieve the corresponding diazonium cations (0.1 M). An excess quantity of hypophosphorous acid (20 ml, 50 %) was added to the solution to reduce the diazonium cations to radicals. GNP (0.1 g) was then dispersed in the solution under stirring for 2 hours to graft the radicals on its surface and obtain $^{COOH-}$GNP. Afterwards, $^{COOH-}$GNP was filtered and washed with deionized water for 10 minutes at least 5 times with ultrasonication.

Amination of Si NP

The surface of Si NP (average diameter of approximately 50 nm, Alfa Aesar) was aminated by anhydrous silane chemistry. As-received Si NP were exposed to air for several hours to ensure the formation of native oxide on its surface. The oxidized Si NP (0.2 g) were dispersed in toluene (10 mL) and (3-aminopropyl)trimethoxysilane (APS, 2 mL, Aldrich) with N_2 as protective gas for 24 h under stirring. Afterwards, the Si NP were separated by centrifugation, washed with toluene and ethanol at least 5 times, and dried under reduced pressure. The modified Si NP is denoted as $^{NH_2-}$Si.

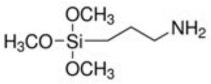

Scheme A1 Chemical structure of (3-aminopropyl)trimethoxysilane

Covalent coupling of $^{NH_2-}$Si and $^{COOH-}$GNP

$^{COOH-}$GNP (0.1 g) was dispersed in a solution of 1.5 g of *N*-(3-dimethylaminopropyl)-*N′*-ethylcarbodiimide hydrochloride (EDC, Fluka) and 0.9 g of *N*-hydroxysuccinimide (NHS, Sigma) in 0.1 L of deionized water. $^{NH_2-}$Si (0.2 g) was then added to the dispersion while stirring, and left overnight. The resulting Si and GNP composite was filtered over 0.8 µm cellulose acetate filter paper (Whatman). The solid was re-suspended in neutral and basic aqueous solutions, ultrasonicated and filtered at least 6 times to ensure that only the covalently attached Si particles remained on the surface of GNP. Since $^{NH_2-}$Si and $^{COOH-}$GNP are both negatively charged in basic pH (inferred from ζ potential measurements), the composite was washed in basic aqueous solution (pH 12) to remove any electrostatically attached NP from $^{COOH-}$GNP. Finally, the composite was dried under reduced pressure, and denoted as Si^{-NHCO-}GNP.

Uncoupled composite, $^{NH_2-}$Si/$^{COOH-}$GNP and Si/GNP

The performance of Si^{-NHCO-}GNP was compared with that of two non-covalently attached Si and graphene composites, $^{NH_2-}$Si/$^{COOH-}$GNP and Si/GNP. To synthesize the electrostatically coupled Si and graphene composite, $^{NH_2-}$Si (0.1 g) was added to $^{COOH-}$GNP (65 mg) dispersed in deionized water by ultrasonication and stirred for 48h. The weight ratio of $^{NH_2-}$Si and $^{COOH-}$GNP was adjusted at 3:2. This ratio was taken after performing thermo-gravimetric analysis of Si^{-NHCO-}GNP, to obtain similar Si weight % in the composites. The pH of the solution was adjusted at 6 to enable electrostatic attraction between $^{NH_2-}$Si and $^{COOH-}$GNP. In this case, EDC and NHS were not added. The composite was dried under reduced pressure and denoted as $^{NH_2-}$Si/$^{COOH-}$GNP. The composite Si/GNP was prepared by dispersing Si (0.1 g) and GNP (65 mg) in ethanol by ultrasonication and stirring for 48 h for uniform mixing. The resulting composite was dried under reduced pressure.

Preparation of Si^{-NHCO-}HOPG and $^{NH_2-}$Si/$^{COOH-}$HOPG

The covalent coupling between NP and graphene in Si^{-NHCO-}GNP using EDC and NHS was confirmed by a control experiment. Highly ordered pyrolitic graphite (HOPG, SPI Supplies grade II) was used as model for GNP and functionalized with –COOH groups following the procedure described above, and denoted as $^{COOH-}$HOPG. A $^{COOH-}$HOPG sample (1mm×1mm) was immersed in an aqueous solution (0.1 L) containing EDC (1.5 g) and NHS (0.9 g), and $^{NH_2-}$Si NP (0.2 g) were added in the solution. Another $^{COOH-}$HOPG sample was immersed in a solution containing only $^{NH_2-}$Si NP (0.2 g), without EDC or NHS. After 24 h, the samples were removed and cleaned using the procedure employed for GNP.

Preparation of Si^{-NHCO-}GO

The spectroscopic evidence of amide bond formation between NP and graphene in using EDC and NHS was provided by a control experiment. The aqueous solution of ultra high concentrated single-layer graphene oxide (GO, Graphene Supermarket, USA) was diluted to a concentration of 1mg/mL. EDC (1.5 g), NHS (0.9 g), and $^{NH_2-}$Si NP (0.2 g) were added to 100 mL of GO solution and stirred for 24 h. The mixture was removed and cleaned using the procedure employed for GNP. The sample was dried under reduced pressure and denoted as Si^{-NHCO-}GO.

Structural characterization

XPS, TGA, ζ potential measurement, SEM, TEM, XRD and FTIR

X–ray photoelectron spectroscopy (XPS) was performed with a monochromatic X–ray photoelectron spectrometer K Alpha (Thermo Scientific), equipped with an Al Kα X–ray source (1486.6 eV). Survey scans and high resolution scans were collected with energy steps of 1 and 0.1 eV, respectively. The spectral energies were calibrated by setting the binding energy of the C 1s component corresponding to C=C–C bonds to 284.4 eV. Thermogravimetric analysis (TGA) was carried out on a Q500 (TA Instruments) at a heating rate of 20°C/min in air. ζ potential analysis of aqueous solutions was performed with a zeta sizer Nano ZS (Malvern Instruments). Electron micrographs were recorded on Jeol JSM7600F and Hitachi SU3500 scanning electron microscopes (SEM) and a Philips CM200 transmission electron microscope (TEM) operated at 200 kV. Powder X-ray diffraction (XRD) was performed on a Bruker D8 Discover system with Co Kα (λ=1.78896 Å) radiation. Attenuated total reflectance – Fourier transform infrared (ATR-FTIR) spectra were taken at room temperature on a Bruker Tensor 27 IR spectrometer using a single pass Ge crystal at an incident angle of 60°.

Quantification of $-NH_2$ groups

A previously described colorimetric method was used to estimate the number of $-NH_2$ groups on the surface of Si NP in Si^{-NHCO-}GNP and $^{NH_2-}$Si/$^{COOH-}$HOPG composites.[1] Ninhydrin assay is widely used to quantify the number of amino groups in biomolecules such as amino acids, proteins and polysaccharides etc. In this assay, ninhydrin reagent is allowed to react with free amino groups to yield a colored compound. The amount of colored compound is measured using UV-Vis absorption spectrometry which in turn gives an estimate of the quantity of amino groups present in the sample. In a typical experiment, first, a calibration curve was obtained by reacting different amounts (0-5 mg) of glycine (Sigma Aldrich) with 2 ml of a 2 w/v% solution of ninhydrin reagent (Sigma Aldrich). The mixture was boiled at 100 °C for 20 minutes. The absorbance of the resulting solution was measured at λ_{max}=570 nm using a UV-Vis spectrophotometer (UV Cary 5000, Varians Inc.). Next, 2 mg of the composite $^{NH_2-}$Si/$^{COOH-}$HOPG was reacted with 2 ml of ninhydrin at 100 °C for 20 minutes. The amount of $-NH_2$ groups present in the sample was calculated by comparing the absorbance on the standard calibration curve. The same procedure was adopted to measure the amount of unreacted $-NH_2$ groups in the composite Si^{-NHCO-}GNP.

Quantification of –COOH groups

To estimate the amount of –COOH groups present on GNP in the Si^{-NHCO-}GNP and $^{NH_2-}$Si/$^{COOH-}$HOPG composites, a previously reported method relying on complexation between transition metal ions and –COOH groups was used.[2] The quantity of free metal ions is determined by adding an indicator which gives a specific red color upon reacting with the metal ions, which is then measured using UV-Vis absorption spectroscopy. Pyrocatechol violet (PV), nickel (II) perchlorate hexahydrate ($Ni(ClO_4)_2 \cdot 6H_2O$), and *N*-(2-Hydroxyethyl) piperazine-*N′*-(2-ethanesulfonic acid) (HEPES) were obtained from Sigma Aldrich and used as received. First, Ni^{2+} stock solutions of varying concentrations (0-200 µM) were prepared in 10mM HEPES (pH 7.5). The solutions were then mixed with 40 µM PV solution prepared in 10mM HEPES. The absorbance of the resulting mixture at λ_{max}= 650 nm was measured immediately using a UV-Vis spectrophotometer (UV Cary 5000, Varians Inc.). A calibration curve was obtained by plotting the absorbance at λ_{max}= 650 nm as a function of Ni^{2+} concentration. To estimate the amount of –COOH groups present on GNP in $^{NH_2-}$Si/$^{COOH-}$HOPG, samples were incubated with 200 µM solution of Ni^{2+} for 2 minutes at room temperature. The mixture was then centrifuged at 12000 rpm and the supernatant was recovered. The supernatant was mixed with 40 µM PV solution in 10mM HEPES. The absorbance at λ_{max}= 650nm was immediately measured and compared with the standard calibration curve to estimate the amount of Ni^{2+}, and in turn of –COOH groups present in the sample.[2] A similar procedure was used to estimate the unreacted –COOH groups in the composite Si$^{-\text{NHCO}-}$GNP.

Anode preparation and cycling

Working anodes composed of Si$^{-\text{NHCO}-}$GNP, ${}^{\text{NH}_2}$–Si/$^{\text{COOH}-}$GNP, Si/GNP and bare Si NP were prepared using a slurry method with sodium alginate as binder (20 % by weight) and Cu foil as current collector. Carbon black (10 % by weight) was also added to bare Si NP to improve the conductivity. The loading of the composites materials was ~0.6 mg/cm^2 of the current collector. CR 2032 coin cells were fabricated in an Ar filled glove box with the working anodes and the Li metal as the reference and counter electrode. Microporous tri-layered polypropylene (PP) and polyethylene (PE) polymer membrane (Celgard, USA) and 1 M $LiPF_6$ in a mixed solution of ethylene carbonate and dimethyl carbonate (1:1 volume ratio, Novolyte, USA) were selected as the separator and electrolyte, respectively. Galvanostatic charging and discharging was carried out for 100 cycles between 0.05 and 1.5 V with a current density of 231 mA g^{-1} for Si$^{-\text{NHCO}-}$GNP, ${}^{\text{NH}_2}$–Si/$^{\text{COOH}-}$GNP and Si/GNP, and 360 mA g^{-1} for Si, corresponding to C/10 rate based on the weight of the active materials, with a formation cycle at C/20.

SI2.Supplementary Results

Fourier transform infrared spectroscopy (FTIR)

We measured ATR-FTIR spectra of all samples to further characterize them, and to get confirmation of covalent coupling. The spectrum of ${}^{\text{NH}_2}$–Si shows two extra features compared to those of Si (compare the red spectra at the bottom of Fig. A1); these both confirm the successful functionalization of the ${}^{\text{NH}_2}$–Si powder, since the peaks appearing between 2830 and 2970 cm^{-1} can be associated to the C–H stretch vibrations and those appearing at ~1100 cm^{-1} can be associated to C–N stretch vibration.[3] The spectra of the three composite materials (Si$^{-\text{NHCO}-}$GNP, ${}^{\text{NH}_2}$–Si/$^{\text{COOH}-}$GNP and Si/GNP, black spectra in Fig. A1) do not reveal structural differences as the Drude conductivity of the composites obscures the amide II signal.

Spectroscopic evidence of amide II bond formation between Si NP and graphene is provided by the spectra of Si$^{-\text{NHCO}-}$GO. Here GNP is replaced by GO to reduce the conductivity of the composite. The amide II bond peak is visible at 1566 cm^{-1} on the FTIR spectrum of Si$^{-\text{NHCO}-}$GO. This peak is clearly not present either in the spectrum of GO, or in the spectrum of ${}^{\text{NH}_2}$–Si powder.

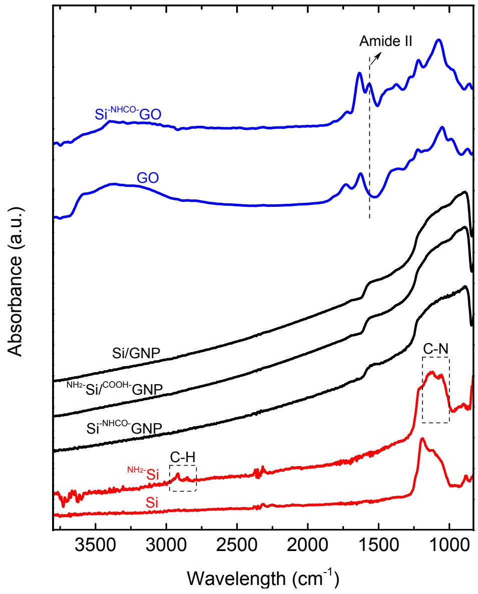

Fig. A1 ATR-FTIR spectra of Si and NH2–Si (red), the three Si and GNP composite anode materials (black), GO and Si$^{-\text{NHCO}-}$GO (blue).

Thermogravimetric analysis (TGA)

TGA curves of GNP and $^{\text{COOH}-}$GNP are shown in Fig. A2a. TGA of GNP shows that burning of graphene takes place between ~500 and 700 °C in the presence of oxygen. The TGA curve of $^{\text{COOH}-}$GNP shows an additional weight loss of up to 6.2 % between 200 and 400 °C in comparison with GNP, which has to be related to the presence of functional groups on GNP. TGA of Si indicates weight increase at temperatures above 500 °C due to the oxidation of Si (Fig. A2b). The weight gain for Si at 500 °C is 1 %. By comparison, the TGA of ${}^{\text{NH}_2}$–Si shows a weight loss of 2.8 % between 50 and 500 °C due to the decomposition of APS functionalities. The difference between weight % for Si and ${}^{\text{NH}_2}$–Si at 500 °C is 3.8 % which corresponds well with the estimated weight % of the functional groups on Si. TGA curves for ${}^{\text{NH}_2}$–Si/$^{\text{COOH}-}$GNP and Si/GNP show ~62 % Si by weight in the composites (Fig. A2c).

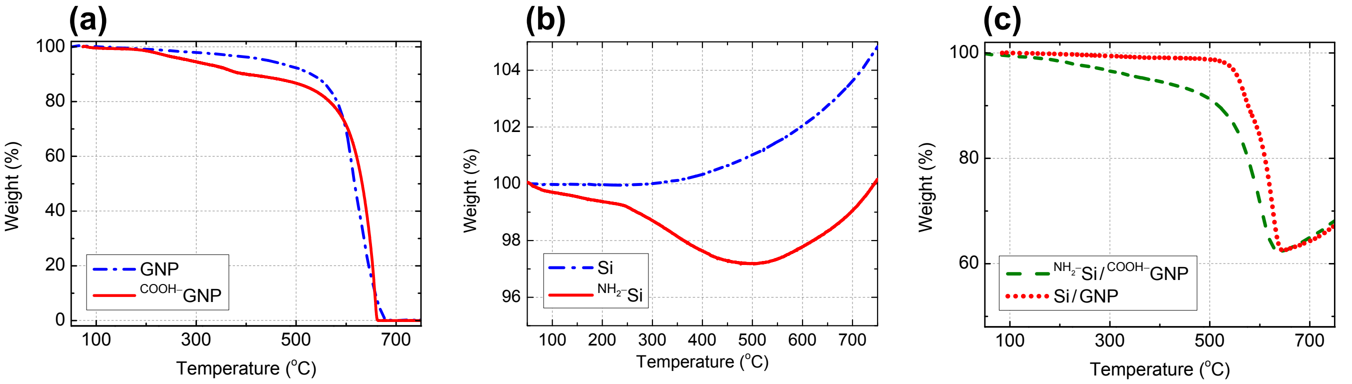

Fig. A2 TGA curves of GNP and $^{COOH-}$GNP in (a), Si and ^{NH_2}–Si in (b), and ^{NH_2}–Si/$^{COOH-}$GNP and Si/GNP in (c).

Surface composition of the anode materials

The surface elemental analysis of the four anode materials is provided in Table A1.

Table A1 Surface elemental analysis (in atomic %) of the composite materials measured by XPS.

	Si (at. %)	O (at. %)	C (at. %)	N (at. %)
Si	61 ± 1	33 ± 1	6 ± 1	
Si^{-NHCO-}GNP	8 ± 1	12 ± 1	77 ± 1	1.8 ± 0.3
$^{NH2-}$Si/$^{COOH-}$GNP	8 ± 1	12 ± 1	78 ± 1	1.7 ± 0.2
Si/GNP	11 ± 1	10 ± 1	79 ± 1	

Transmission electron microscopy (TEM)

TEM of GNP reveals that the thickness of GNP is ~2-3nm (7-10 graphene layers), and the TEM images of the composite, Si^{-NHCO-}GNP, ^{NH}$_2$–Si/$^{COOH-}$GNP and Si/GNP, and bare Si show 2-3 nm thick SiO_x around Si (Fig A3).

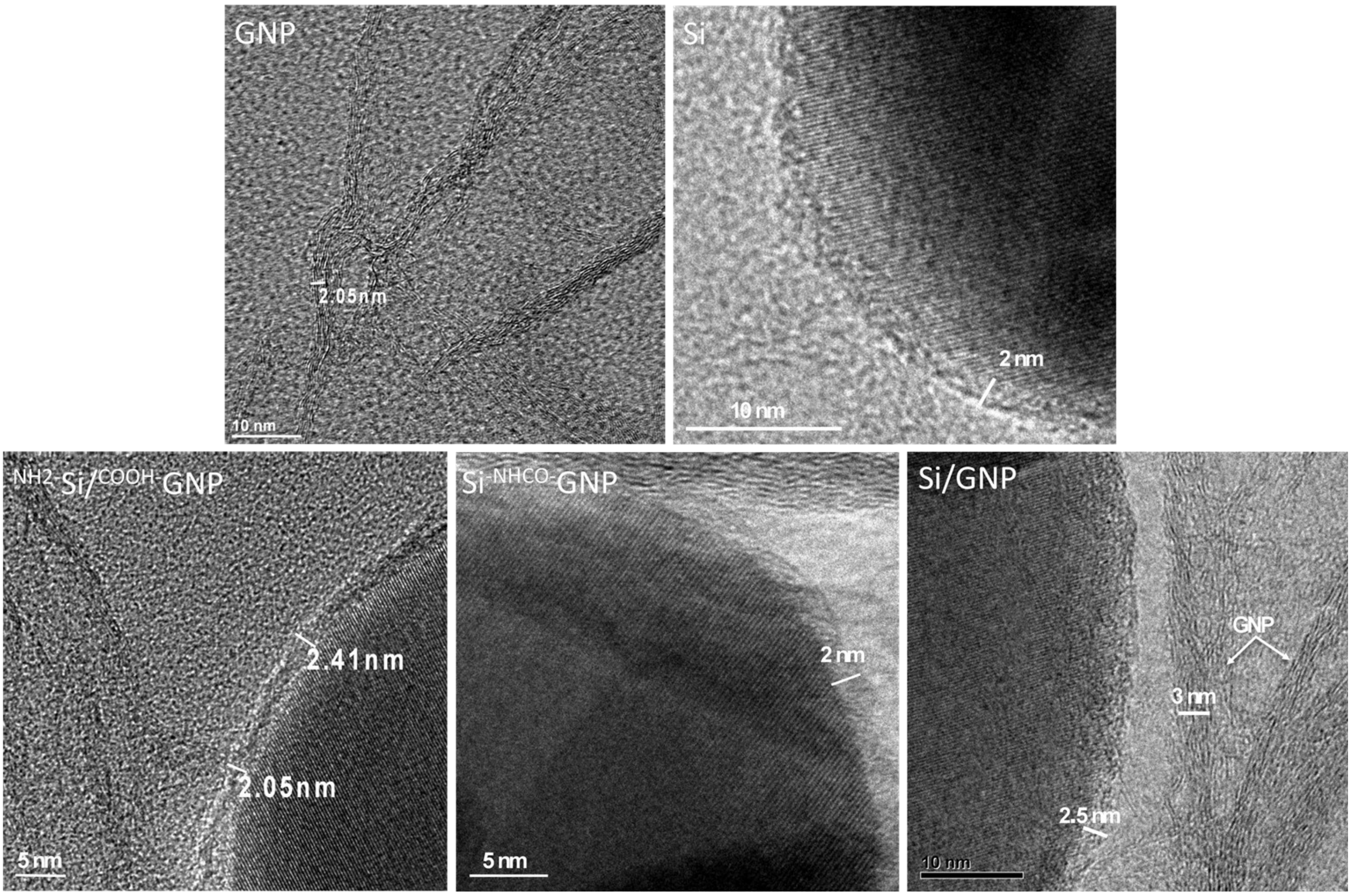

Fig. A3 TEM images of GNP, Si and the composites ^{NH}$_2$–Si/$^{COOH-}$GNP, Si^{-NHCO-}GNP and Si/GNP.

Scanning electron microscopy (SEM) and X-ray diffraction (XRD) of Si^{-NHCO-}GNP

The SEM image of Si^{-NHCO-}GNP (Fig. A4a) shows the attachment of Si NP of on the crumpled structure of $^{COOH-}$GNP. The carboxylic functional groups on GNP act as anchors for NP immobilization. The diffraction pattern of the Si^{-NHCO-}GNP composite is shown in Fig. A4b. The broad peak centred at ~31° is related to the (002) diffraction of graphitic layers in GNP. Other peaks located at 33.1°, 55.5°, 66.2° and 82.5° are associated with the (111), (200), (311) and (400) diffractions of Si, respectively.

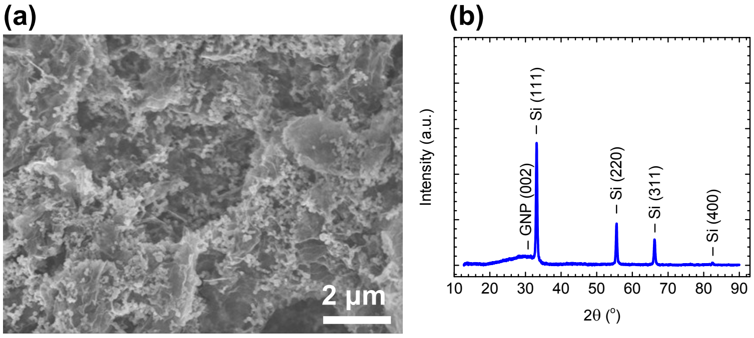

Fig. A4 SEM (a), and XRD pattern (b) of Si^{-NHCO-}GNP composite.

Theoretical capacity calculation

Table A2 Estimated theoretical capacities for Si and the composite anodes

	Si (wt %)	C (wt %)	Theoretical Capacity (mAh g^{-1})*	C/20 (1st cycle)	C/10 (2nd-100th cycle)
Si	100	0	3600	180	360
Si^{-NHCO-}GNP	60	40	2309	115	231
$^{NH2-}$Si/$^{COOH-}$GNP	62	38	2388	119	239
Si/GNP	62	38	2388	119	239

Theoretical capacity of Si = 3600 mAh g^{-1}, C = 372 mAh g^{-1}

* Note that this value is an overestimate because the presence of silicon oxide and other functional layers are not accounted for.

Anode cycling tests

Table A3 The 1st (formation), 2nd and 100th cycle specific discharge and charge capacities, Coulombic efficiencies and capacity retention for Si and the composite anodes

Anode material	cycle # 1			cycle # 2				cycle # 100			
	discharge capacity (mAh g^{-1})	charge capacity (mAh g^{-1})	Coulombic efficiency (%)	discharge capacity (mAh g^{-1})	charge capacity (mAh g^{-1})	Coulombic efficiency (%)	capacity retention (%)	discharge capacity (mAh g^{-1})	charge capacity (mAh g^{-1})	Coulombic efficiency (%)	capacity retention (%)
Si	2262.3	1759.7	77.8	1491.1	1069.7	71.7	60.8	279.3	278.2	99.6	15.8
Si^{-NHCO-}GNP	2120.9	1634.5	77.1	1600.5	1546.2	96.6	94.6	897.6	891.0	99.3	54.5
^{NH_2}-Si/$^{COOH-}$GNP	2111.5	1112.0	52.7	1043.3	943.0	90.4	84.8	44.7	43.1	96.3	3.9
Si/GNP	2236.5	1542.9	69.0	1369.9	1307.2	95.4	84.7	226.0	221.5	98.0	14.4

Differential capacity plots

The 1st, 2nd and 10th cycle differential capacity plots for Si^{-NHCO-}GNP within a voltage window of 0.05–1.5 V vs Li are shown in Fig. A5. Only a single peak between 0.05 V and 0.16 V is observed at ~0.1 V on the 1st discharge half cycle. Two electrochemical reactions are anticipated in this voltage range for Si. First, the formation of amorphous Li_xSi from crystalline Si (~0.1 V)[4] and next a phase transition from amorphous Li_xSi to crystalline $Li_{15}Si_4$ (0.07 V).[5] The lithiation of graphene usually takes place below 0.1 V,[5] and may have contributed to the observed peak broadening. On the subsequent lithiation half cycles, an additional peak at 0.23 V emerges, which we attribute to higher voltage lithiation of amorphous Li_xSi.[4] The delithiation peaks at 0.27 V and 0.47 V are related to the phase transition between crystalline Li_ySi to amorphous Li_xSi, and amorphous Li_xSi to amorphous Si, respectively. The expected graphene delithiation peak around 0.2 V is too small to be observed, suggesting a low contribution of graphene to the overall anode capacity. The lithiation and delithiation peak intensities in the 10th cycle are similar to those in the 2nd cycle which indicate stable reversible electrochemical reactions at the anode.

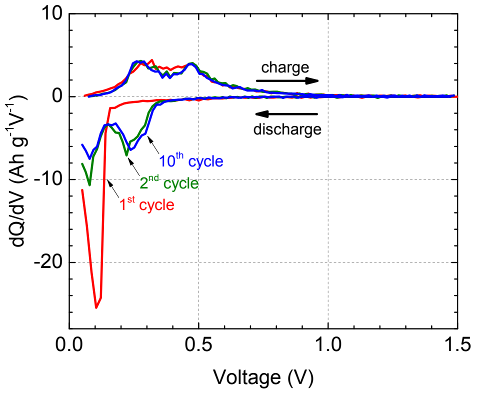

Fig. A5 dV versus voltage for the 1st (formation), 2nd and 10th cycles of the Si–NHCO–GNP anode

Scanning electron microscopy of the anodes before and after cycling

The SEM images of the Si and the composite anodes before and after cycling are shown in Fig. A6. The morphology of the three composite electrodes after cycling is very similar and the solid electrolyte interphase (SEI) films, which form due to the decomposition of the electrolyte, are continuous on the anode surfaces. This seems to imply that the capacity fading in the uncoupled electrode is mainly due to the electric isolation of the Si particles due to the absence of bond between Si and graphene. In the case of bare Si, large cracks and discontinuous SEI film is observed after cycling, which can be explained through fracture induced by the large volume change of Si during cycling.

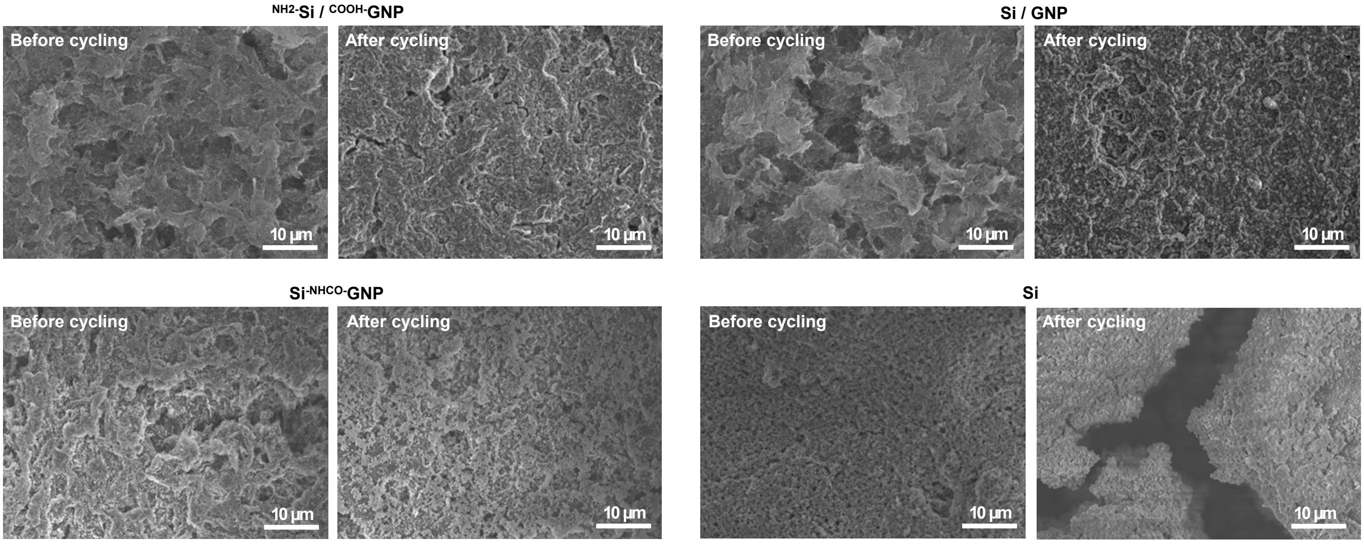

Fig. A6 SEM images of the bare Si and the composite anodes before and after cycling

References

1. L.-P. Yan, Y.-J. Wang, L. Ren, G. Wu, S. G. Caridade, J.-B. Fan, L.-Y. Wang, P.-H. Ji, J. M. Oliveira, J. T. Oliveira, J. F. Mano and R. L. Reis, *Journal of Biomedical Materials Research Part A*, 2010, **95A**, 465-475.
2. A. Hennig, A. Hoffmann, H. Borcherding, T. Thiele, U. Schedler and U. Resch-Genger, *Analytical Chemistry*, 2011, **83**, 4970-4974.
3. S. A. McCarthy, G.-L. Davies and Y. K. Gun'ko, *Nature protocols*, 2012, **7**, 1677-1693.
4. A. Magasinski, P. Dixon, B. Hertzberg, A. Kvit, J. Ayala and G. Yushin, *Nature Materials*, 2010, **9**, 353-358.
5. S.-L. Chou, J.-Z. Wang, M. Choucair, H.-K. Liu, J. A. Stride and S.-X. Dou, *Electrochemistry Communications*, 2010, **12**, 303-306.